

Direct Electrochemistry of Drug Metabolizing Human Flavin-Containing Monooxygenase: Electrochemical Turnover of Benzylamine and Tamoxifen

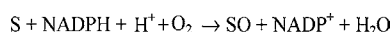
Sheila J. Sadeghi,[†] Rita Meirinhos,[†] Gianluca Catucci,[†] Vikash R. Dodhia,[‡] Giovanna Di Nardo,[†] and Gianfranco Gilardi^{*†‡}

Department of Human and Animal Biology, University of Turin, Italy, and Division of Molecular Biosciences, Imperial College London, U.K.

Received October 31, 2009; E-mail: g.gilardi@imperial.ac.uk

Human flavin-containing monooxygenase 3 (hFMO3) is a microsomal phase I drug metabolizing enzyme that catalyzes the oxygenation of a wide range of nitrogen- and sulfur-containing drugs as shown in Scheme 1 (where S is the substrate).¹ In general, research on electrochemical catalysis of drug-metabolizing monooxygenases has been mainly confined to cytochrome P450 enzymes with FMO largely neglected. FMO studies have been limited to Clarke-type dissolved-oxygen electrode settings.² To date there are no reports on direct immobilization strategies of FMO enzymes with electrocatalytic drug turnover.

Scheme 1



Herein we describe the first direct electrochemistry of hFMO3 immobilized on both glassy carbon (GC) and gold electrodes. The enzyme was cloned, expressed, and purified in a soluble, active form in bacteria. GC electrodes were derivatized with the cationic surfactant didodecylammonium bromide (DDAB).³ The protein film was prepared by mixing equal volumes of the protein and surfactant before drop-coating onto the electrode surface. A typical cyclic voltammogram (CV) of hFMO3 is shown in Figure 1A. At room temperature and under anaerobic conditions, the immobilized enzyme showed a single redox couple with a midpoint potential (E_m) of -445 ± 8 mV (vs Ag/AgCl). Integration of the reduction peak from the baseline corrected CV allowed for the calculation of the charge transferred upon reduction of the protein and for the determination of the quantity of the immobilized electroactive protein. The coverage was 2.6×10^{13} molecules per cm^2 indicating a multilayer formation corresponding to roughly 3 layers. Voltammograms of hFMO3 were taken at different scan rates ranging from 10 to 150 mV s^{-1} . The peak-to-peak separation (ΔE_p) of 61 mV did not vary significantly within the mentioned range. Instrumental limitations did not allow for higher scan rates, therefore preventing k_{ET} measurements. Furthermore, peak currents (i_{pc} and i_{pa}) were linearly dependent on the scan rate, suggesting that the quasi-reversible reaction is a surface-controlled process, as expected for an immobilized electroactive species. The electrochemically determined E_m value for hFMO3 immobilized on the GC electrode is in the range of the literature values for other flavin-containing monooxygenases.⁴

The electrochemical response on the gold electrode could only be observed after modification of the surface. Functionalization of the Au surface with dithio-bismaleimidoethane (DTME)⁵ led to the formation of maleimide-terminated groups which can covalently link to hFMO3 via surface exposed cysteine residues. The resulting

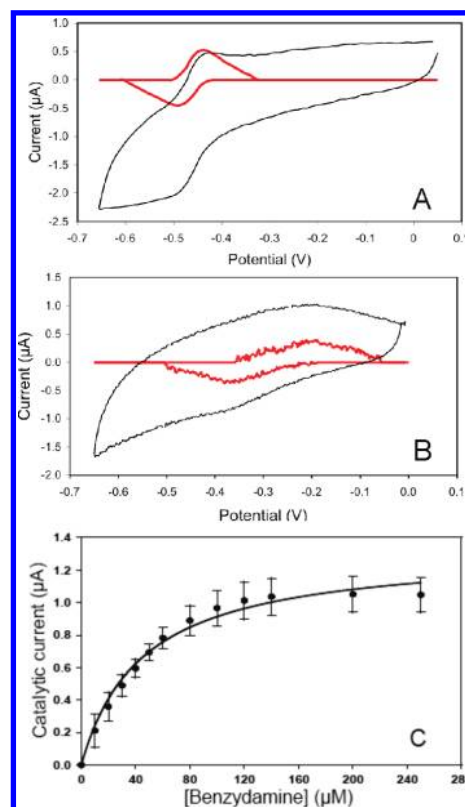


Figure 1. Anaerobic cyclic voltammograms of hFMO3 immobilized on different electrode surfaces: (A) GC/DDAB/FMO3, (B) Au/DTME/FMO3. Scan rate 50 mV/s (A) and 2 mV/s (B) in 100 mM phosphate buffer with 100 mM KCl pH 7.4 at 25 °C. Shown are the original (black) and baseline corrected CVs (red, intensities multiplied by 2 for clarity). (C) Benzylamine titration of GC/DDAB/hFMO3. The error bars represent the estimated standard deviation for the mean of three separate electrode measurements.

covalently immobilized hFMO3 gave two waves with an E_m of -280 ± 12 mV (Figure 1B). This value is ~ 165 mV more positive than the E_m measured for the noncovalently immobilized protein on the GC electrode and could be attributed to the electrode surface and its modifications which have been shown to affect the reduction potentials of other monooxygenases.^{3a,6} The coverage was calculated to be 3.4×10^{12} molecules per cm^2 (Table 1), indicating a submonolayer formation.

The ability of the immobilized hFMO3 to oxygenate two of its known substrates was investigated and compared with solution studies. The first substrate, benzylamine, is a nonsteroidal anti-inflammatory drug shown to be extensively metabolized to its *N*-oxide by hFMO3.^{7,8} The second substrate, tamoxifen, is a widely used antiestrogenic drug for the treatment of breast cancer and has

[†] University of Turin.

[‡] Imperial College London.

been shown to be metabolized by hFMO3 to its *N*-oxide form. However, for this substrate there are also 3 other metabolites produced by cytochromes P450.⁹

Table 1. Redox and Catalytic Parameters of hFMO3 Immobilized on Different Surfaces

electrode	E_m (mV)	no. of molecules/cm ²	tamoxifen <i>N</i> -oxide ^a (μ M)
GC/DDAB/hFMO3	-445 ± 8	2.6×10^{13}	1.65 ± 0.13
Au/DTME/hFMO3	-282 ± 12	3.4×10^{12}	8.03 ± 0.11

^a The concentration of tamoxifen *N*-oxide is normalized by the number of hFMO3 molecules on the electrode.

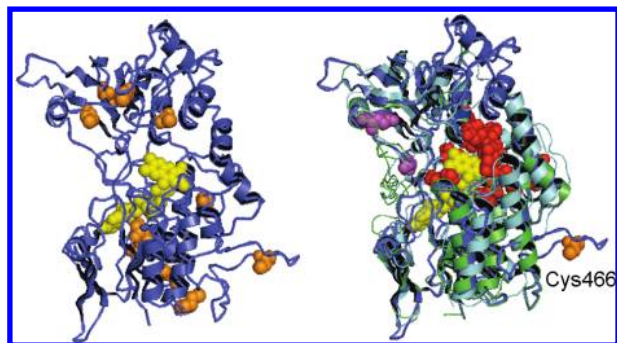


Figure 2. Homology model of hFMO3 with cysteine residues in orange and FAD cofactor in yellow (left). Superimposed structures (right) of yeast (green, PDB:2GV8) and bacterial (cyan, PDB:2VQ7) FMO with hFMO3 model (blue). Residues forming the active site are in red, and the putative access channel in purple.

Bioelectrocatalysis experiments were carried out to assess the catalytic activity of hFMO3 immobilized on both GC and Au electrodes. A potential bias of -600 mV (vs Ag/AgCl) was applied for 30 min to the aerated cell that was continuously stirred. The products formed were analyzed by HPLC where two peaks with retention times of 7.5 and 19.4 min were separated and assigned to tamoxifen *N*-oxide and tamoxifen, respectively. The amount of *N*-oxide formed by the immobilized enzyme during bioelectrochemical catalysis was quantified using a standard curve. The concentrations of the product formed are reported in Table 1. While no *N*-oxide product was detected in the absence of the enzyme, in its presence 1.7 and 8.0μ M of the product were detected on GC/DDAB/hFMO3 and Au/DTME/hFMO3, respectively. This finding supports the evidence that the electrochemical signal is associated to catalytically active immobilized hFMO3.

In comparing the amount of active hFMO3 on both surfaces with the amount of product formed (Table 1) it is obvious that immobilization on the Au surface is more successful in terms of catalysis. This is interpreted with the presence of an oriented layer of hFMO3 that is achieved by covalent linkage via exposed surface cysteine residues. To support this interpretation, a 3D model of the protein was constructed using homology modeling based on the structure of yeast (*S. pombe*) FMO.¹⁰ The model (Figure 2) was used for measuring the accessible solvent area (ASA) of the 11 cysteine residues present in the hFMO3 amino acid sequence. The calculated solvent exposures showed that the majority of the cysteines are hardly accessible with an ASA lower than 9%. As

for the remaining cysteine residues, Cys 466 has the highest exposure of 57% making it the most probable candidate for covalent binding to the maleimide group of DTME. Superimposition of the available crystal structures of bacterial (*Methylophaga*)¹¹ and yeast¹⁰ FMO with the hFMO3 homology model generated here shows that the most exposed cysteine (Cys 466) is indeed located in the opposite side of the access channel to the catalytic site and, therefore, covalent linkage of the Cys 466 to the DTME/Au electrode will favor catalysis.

Finally, the exploitation of hFMO3 using electrochemical techniques is a very attractive prospective for identifying drugs or drug candidates as substrates. To this end, electrochemical titrations of GC/DDAB/hFMO3 with benzydamine in air-saturated buffer were carried out using cyclic voltammetry. The increase in observed catalytic reduction current was subsequently measured for each concentration of benzydamine added. The results shown in Figure 1C indicate that the immobilized enzyme responded to the presence of the substrate in a Michaelis–Menten fashion with a net current at saturation of $\sim 1 \mu$ A. The electrochemical K_M calculated is $44 \pm 5 \mu$ M, which is in good agreement with the values published for microsomal hFMO3 using NADPH as an electron donor.⁸

Acknowledgment. This work has been supported in part by the Marie Curie RTN (35649) project.

Supporting Information Available: Electrode preparations and HPLC experimental setup. This material is available free of charge via the Internet at <http://pubs.acs.org>.

References

- (1) (a) Ziegler, D. M. *Drug Metab. Rev.* **2002**, *34*, 503–511. (b) Krueger, S. K.; Williams, D. E. *Pharmacol. Therap.* **2005**, *106*, 357–387. (c) Cashman, J. R. *Exp. Opin. Drug Metab. Toxicol.* **2008**, *4*, 1507–1521.
- (2) (a) Saito, H.; Kaneko, Y.; Hashimoto, Y.; Shirai, T.; Mitsubayashi, K. *Int. J. Environ. Anal. Chem.* **2006**, *86*, 1057–64. (b) Saito, H.; Kaneko, Y.; Hashimoto, Y.; Shirai, T.; Kudo, H.; Otsuka, K.; Mitsubayashi, K. *Sens. Actuators B* **2007**, *123*, 877–881. (c) Saito, H.; Shirai, T.; Kudo, H.; Mitsubayashi, K. *Anal. Bioanal. Chem.* **2008**, *391*, 1263–68. (d) Fillit, C.; Jaffrezic-Renault, N.; Bessueille, F.; Leonard, D.; Mitsubayashi, K.; Tardy, J. J. *Mater. Sci. Eng. C* **2008**, *28*, 781–786.
- (3) (a) Rustling, J. F. *Acc. Chem. Res.* **1998**, *31*, 363. (b) Fantuzzi, A.; Fairhead, M.; Gilardi, G. *J. Am. Chem. Soc.* **2004**, *126*, 5040–5041.
- (4) (a) Einarsdottir, G. H.; Stankovich, M. T.; Powlowski, J.; Ballou, D. P.; Massey, V. *Biochemistry* **1989**, *28*, 4161–68. (b) Shaw, J. P.; Harayama, S. *Eur. J. Biochem.* **1992**, *209*, 51–61. (c) Sheng, D.; Ballou, D. P.; Massey, V. *Biochemistry* **2001**, *40*, 11156–67. (d) Xie, W.; Jones, J. P.; Wong, L.-L.; Hill, H. A. O. *Chem Commun.* **2001**, 2370–71. (e) Fraaije, M. W.; Kamerbeek, N. M.; Heidekamp, A. J.; Fortin, R.; Janssen, D. B. *J. Biol. Chem.* **2004**, *279*, 3354–60.
- (5) Ferrero, V. E. V.; Andolfi, L.; Di Nardo, G.; Sadeghi, S.; Fantuzzi, A.; Cannistraro, S.; Gilardi, G. *Anal. Chem.* **2008**, *80*, 8438–46.
- (6) (a) Fleming, B. D.; Tian, Y.; Bell, S. G.; Wong, L. L.; Urlacher, V.; Hill, H. A. O. *Eur. J. Biochem.* **2003**, *270*, 4082. (b) Udit, A. K.; Hindoyan, N.; Hill, M. G.; Arnold, F. H.; Gray, H. B. *Inorg. Chem.* **2005**, *44*, 4109. (c) Dodhia, V. R.; Sassone, C.; Fantuzzi, A.; Di Nardo, G.; Sadeghi, S.; Gilardi, G. *Electrochem. Commun.* **2008**, *10*, 1744–1747.
- (7) (a) Catanese, B.; Lagana, A.; Marino, A.; Piccolo, R.; Rotatori, M. *Pharmacol. Res. Commun.* **1986**, *18*, 385–403. (b) Baldock, G. A.; Brodie, R. R.; Chasseaud, L. F.; Taylor, T. *J. Chromatogr.* **1990**, *529*, 113–123.
- (8) (a) Lang, D. H.; Rettie, A. E. *J. Clin. Pharmacol.* **2000**, *50*, 311–314. (b) Stormer, E.; Roots, I.; Brockmoller, J. *J. Clin. Pharmacol.* **2000**, *50*, 553.
- (9) (a) Mani, C.; Hodgson, E.; Kupfer, D. *Drug Metab. Dispos.* **1993**, *21*, 657–661. (b) Krueger, S. K.; VanDyke, D. E.; Hines, R. N. *Drug Metab. Rev.* **2006**, *38*, 139–147.
- (10) Eswaramoorthy, S.; Bonanno, J. B.; Burley, S. K.; Swaminathan, S. *Proc. Natl. Acad. Sci. U.S.A.* **2006**, *103*, 9832–37.
- (11) Alfieri, A.; Malito, E.; Orru, R.; Fraaije, M. W.; Mattevi, A. *Proc. Natl. Acad. Sci. U.S.A.* **2008**, *105*, 6572–77.

JA909261P